Final paper submission: XIV International ISM Congress,
20 September to the 24 September 2010
at Sun City, South Africa

UTILISATION OF INSAR FOR MONITORING OF SUBSIDENCE OVER MINING CAVING ZONES

Hani Zahiri[(1)], Andrew Jarosz[(1)], Andrew Sowter[(2)]

(1) Curtin University of Technology - Western Australian School of Mine, Locked Bag 22, Kalgoorlie WA 6433, Australia,
Tel: +61 8 9088 6163,
Fax: +61 8 9088 6151,
Email: a.jarosz@curtin.edu.au

(2) The University of Nottingham - Institute of Engineering Surveying and Space Geodesy, University Park Nottingham NG7 2RD, United Kingdom, Email: Andrew.Sowter@nottingham.ac.uk

Abstract

The utilisation of InSAR techniques for the monitoring of subsidence over mining areas, employing open pit and underground mining methods, has a large potential due to inaccessibility and safety issues associated with the usage of classical surveying techniques. InSAR can also be very competitive concerning the cost of provided results. However, there are a few issues that may significantly limit InSAR applicability for subsidence monitoring in mining areas. The highly dynamic character of subsidence induced by mining, especially employing caving as a mining system, may lead to ambiguity issues. This could happen when the vertical movement between the neighbouring cells (pixels) of the SAR image is greater than quarter of the wavelength of a radar signal over the period between image acquisitions. The altered terrain topography, involving steep slopes and deep pits, may also lead to radar signal layover issues for specific satellite and pit slope geometry.

In this paper the authors analyse the above-mentioned issues and present how the InSAR technology was applied as a help to monitor large scale and highly dynamic subsidence for a real case study in Western Australia. It was recognised that the analysis of ground deformation dynamics, based on topographical surveys, may provide a basis for the resolution of ambiguity issues existing in InSAR processing. Also, the new technique involving generation of a detailed DEM based on the current topographical surveys and pixel-by-pixel analysis were applied in order to identify a precise extent of layover areas.

Key Words: subsidence, caving, mine deformation, InSAR, GIS, remote sensing

1. Introduction

The instability of mine slopes is a source of risk for people, equipment and the environment. It may also disrupt scheduling and increase the cost of mine safety and production (Lilly et al., 2000). Consequently, a comprehensive knowledge of the mechanisms associated with rock strata deformation is crucial for any mining activity. This is of particular importance for planning, as the impact of induced caving on the surface and surrounding infrastructure needs to be understood, to allow for a management program (and risk mitigation) to be developed and implemented. A better understanding of rock strata deformation mechanisms requires the collection of accurate displacement data over the area affected. Classical techniques have notable disadvantages that limit their applicability, particularly in terms of coverage, repeatability, risk and accuracy. They follow point-by-point data collection techniques and therefore are relatively time-consuming

and costly. Surveys usually cover only a small area and produce much localised information. Furthermore, classical techniques are not applicable for the monitoring of inaccessible areas and since monitoring points are not close enough, they are not able to provide a reliable interpolation of data (Ge et al., 2004). Considering this, there is increasing demand to design and utilise cost-efficient supplementary or alternative techniques with the capability to deliver continuous coverage and accuracies, comparable or exceeding that of classical surveys. By using Interferometric Synthetic Aperture Radar (InSAR) a localised surface subsidence may be monitored to sub-centimetre accuracy. InSAR does not require any field instrumentation and consequently allows for monitoring of hazardous and inaccessible areas. A Geographical Information System (GIS) or any other spatial processing software can easily further process the InSAR results, which can be utilised to provide a valuable calibration tool for rock strata deformation models. Utilisation of the InSAR technique significantly reduces the costs of the subsidence monitoring and interpretation process.

In spite of the wide application of InSAR techniques for the monitoring of large-scale deformations of the Earth crust, specific modifications are necessary for utilising the technology in a mining context. Limitations, such as a difficulty to resolve deformation for a high gradient slope, a difficulty to retrieve subsidence for localised highly dynamic ground movements and the unavailability of SAR images with the desired specifications, restrict the potential to monitor high rate, localised mine subsidence on day-to-day basis (Wegmüller et al., 2005).

In this paper the authors analyse the above-mentioned issues and present how the InSAR technique can be applied to the monitoring of large scale and highly dynamic subsidence for a real case study in Western Australia. The primary focus of the paper will be on the Perseverance open pit and underground mine. This mine is a part of BHPBilliton‘s Leinster Nickel Operation, located 645 kilometres north-east of Perth in Western Australia. Western Australia’s climate conditions, of dry cloudless weather with minimal atmospheric disturbances, are conducive to obtaining good quality SAR based interferograms. However, the vast mostly uninhabited area of Western Australia is not a primary target of SAR missions, whence archived data is scarce and without any continuity. As will be described below, the authors found only a very small number of SAR acquisitions in the archive (there were only10 ERS-2 SAR images gathered after 2000). Furthermore, considering acquisitions geometry, only data from descending orbits was available.

As described above, the topography of a mine does cause some prospective problems that can drastically reduce the amount of good results possible when using InSAR. In this paper, we describe a new technique for the geometrical interpretation of a mine site that involves the generation of a detailed DEM based on current topographical surveys and a pixel-by-pixel analysis to identify the precise extent of the poorly described areas. A comprehensive analysis of ground deformation dynamics, based on topographical surveys has also been carried out in order to determine which InSAR results may be affected by ambiguity issues. This analysis may provide a basis for further adjustment of extend of poorly described areas.

2. Layover Analysis

Layover is commonly seen in SAR imagery containing severe terrain variations. It occurs when the top of a topographic feature is actually closer (of smaller slant-range) than features on the slopes. This results in the superposition of large areas into only small numbers of pixels in the slant range image; this situation means layover pixels are useless for interferometric analyses.

Figure 1 illustrates the geometry of the descending ERS orbit geometry for the case study. ERS is viewing the pit from the East at an incidence angle of approximately 23º. The satellite sends out short, high energy, pulses and listens for the response; ideally, the oblique incidence angle of the satellite means that only one response from each target on the ground will be received and that, therefore, responses from adjacent targets will not be confused. As can be seen from the figure, this is not the case on the Western side of the pit where the radar wavefronts are striking three points simultaneously: on the floor of the pit; on the Western wall; and on the surface. This means that, in the SAR image, all three points will be superimposed, forming a very thin but bright area in the image. This is a region of Layover and the superposition of targets means that an interferometric signal cannot be discriminated, making it a useless area for the analysis.

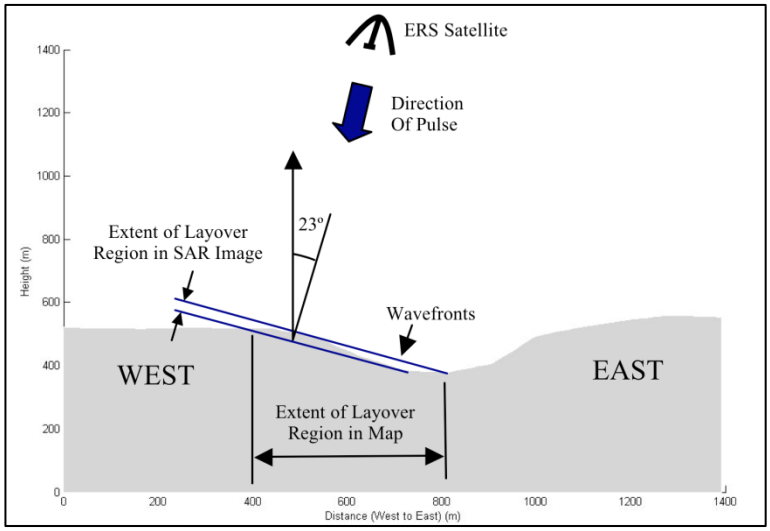

Figure 1: Height profile across the pit indicating the layover scenario

Figure 1 also illustrates that, although a layover region appears small in a SAR image, its extent on the ground can be very large indeed. In our case, the layover effect covers an area extending some 400m across the ground, eliminating the Western half of the pit and a large part of its edge from the interferometric analysis.

When undertaking the InSAR analysis, it was important to identify the precise extent of the layover area as part of this analysis. In theory, at least, identifying a layover pixel in an image should be simple, assuming a model of the terrain is available, as the criterion is actually very easy– if more than one position on the ground maps to the same pixel in the image, then that pixel is in layover. In practice, this is very difficult to implement as the relative size of pixels in relation to the sampling of DEM postings could result in more than one posting mapping to the same pixel without being in layover. A better algorithm is to work along the path of an image range line along the ground and calculate the change in slant range from posting to posting. If the slant range increases, the pixel is not in layover; if it decreases then the pixel is in layover and every subsequent pixel is too, until the first slant range value is restored.

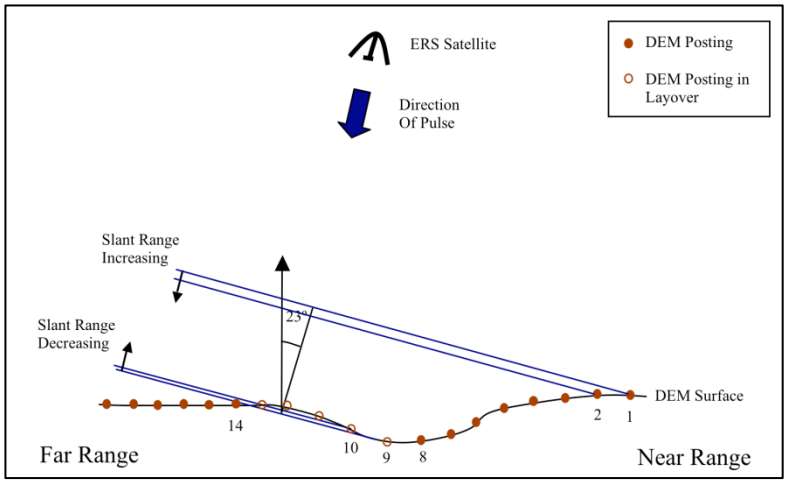

Figure 2: Estimating the layover from the DEM postings

An example of this type of algorithm is shown in **Figure 2**. The satellite-ground geometry of each DEM posting along a range line is calculated starting at the near-range position and working along each point in turn towards the far range direction. The change in slant range from point-to-point is calculated. If slant range increases, as for points 1 and 2 in the figure, this is consistent with there being no layover present; when it decreases between adjacent points, as for points 9 and 10, there is layover. In fact, for the latter case, point

9 represents the start of a layover region: all points after that will be labelled as layover until the original slant range value at 9 is restored. In this instance, point 14 is the first point to emerge from the layover region. Once a layover region has been identified using this algorithm, there is some tidying up to do to make sure that some points do not slip through the net. For example, point 8 may be in the layover region if it has a slant-range between the maximum and minimum values covered by the layover area.

The most difficult part of this task, though, is to identify where each image range line falls on the terrain model. In the analysis undertaken here, a backwards geocoding algorithm, using range and Doppler equations along with a satellite model (Schreier, 1993), was implemented to determine the range line number of every DEM posting. Then, each range line was traced in turn, calculating the slant range along the path from near to far range. Every layover pixel could then be identified in the slant range image. This resulted in a layover mask for the slant range image. To identify the same areas in ground range, the layover mask was then geocoded to a map frame.

2.2 Effects of using current DEM for Layover analysis

Initial analyses of the layover mask suggested that the SRTM DEM can sufficiently describe the terrain topography current at the acquisition time of the ERS SAR images for the Leinster mine (see Section 3.2); however this is definitely not the case for more recent case studies. The SRTM DEM was generated from data acquired during 2000 (Farr et al., 2007). Therefore, those sites that have experienced significant changes in topography between 2000 and the dates of the SAR acquisitions may find that the SRTM DEM is not accurate enough. In such cases, utilising a more current DEM must be considered to include more recent topographical changes into the analysis. In order to illustrate the effect of employing current DEM against SRTM DEM for layover analysis, we briefly discuss another case study, Argyle Diamond Mines located in North of Western Australia. The analysis for this site carried out utilised ENVISAT SAR images with a 7-year gap between the SRTM observations and the acquisitions of the ENVISAT images. During this time, due to extensive mining activities, noticeable changes of the topography occurred around and inside the pit. The appearance of the pit in the slant-range SAR image is shown in **Figure 3**. In this image, ENVISAT is viewing the geometry from the left of the illustration so the Western wall of the pit is very clear on the left of the image.

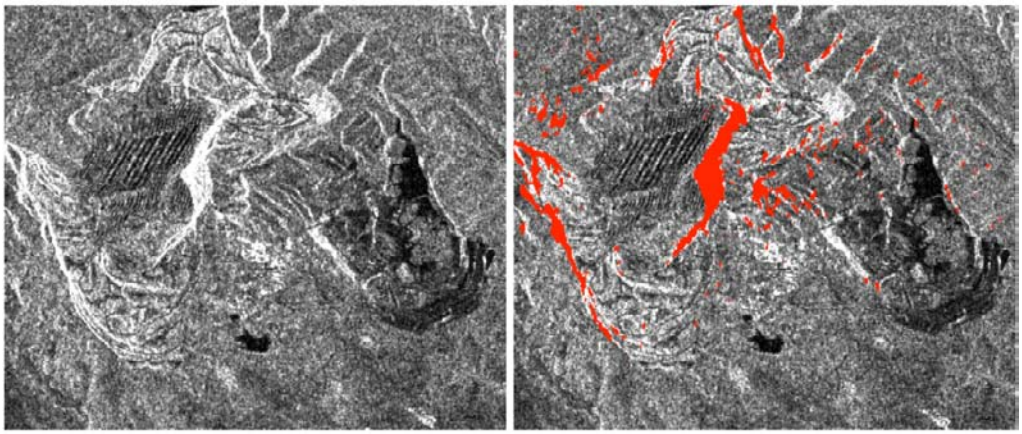

Figure 3: A slant range SAR image of Argyle Diamond Mines

The results of geocoding and layover masking using the SRTM DEM and the most current DEM are shown in **Figure 4** and **5** respectively. Inspection of the figure indicates that the SRTM DEM has only partly been able to rectify the image and that the areas we would expect to be smoothly rectified are instead strangely shaped and with inconsistencies in them. For example, the layover area on the Eastern side of the wall still retains some of the sigmoid shape in the original SAR image (see **Figure 3**) and there is a dark “hole” in its centre, consistent with there being a mis-match between the simulated distortion and the distortion in the image. The layover mask, although roughly in the correct position, is also strangely shaped and does not match the shape of the bright pixels, which is further evidence that the SRTM DEM is not describing the mine topography properly.

We now know that there have been enormous (see Section 4.2.2 and Figures 13 and 14) changes in topography over the study area due to substantial mining activities between 2000 and 2007. To this end a new, limited extent, DEM representing these changes was created using a digital terrain model (DTM) generated from up-to-date classical and photogrammetric surveys. To integrate the new, smaller DTM with the much larger SRTM DEM, the larger DEM was re-sampled, as the new DTM has much higher resolution and covers more details, and the elevation values over the mine site were replaced with values from the new elevation model. The final product is a high resolution DEM with up-to-date elevation values. The use of an appropriate re-sampling method, that avoids creation of a terrace effect at the boundaries of insertion area, was crucial. The new regenerated DEM has been used for creation of a new layover mask and in the final InSAR processing. This was used to generate the final SAR products and is shown in **Figure 4**. It is clear from the comparison of Figure 4 and **5** that a detailed DEM leads toward much more accurate layover mask and therefore better confidence in the InSAR results.

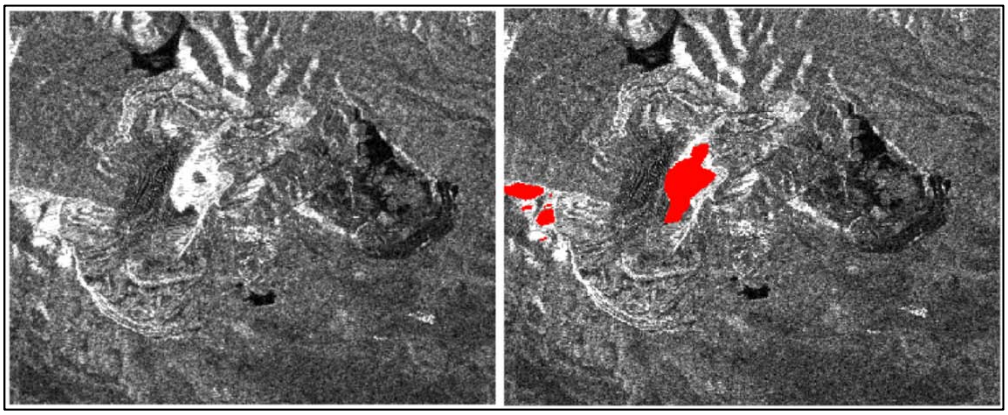

Figure 4: A geocoded SAR image of Argyle Diamond Mines (left) and with layover area highlighted in red (right)

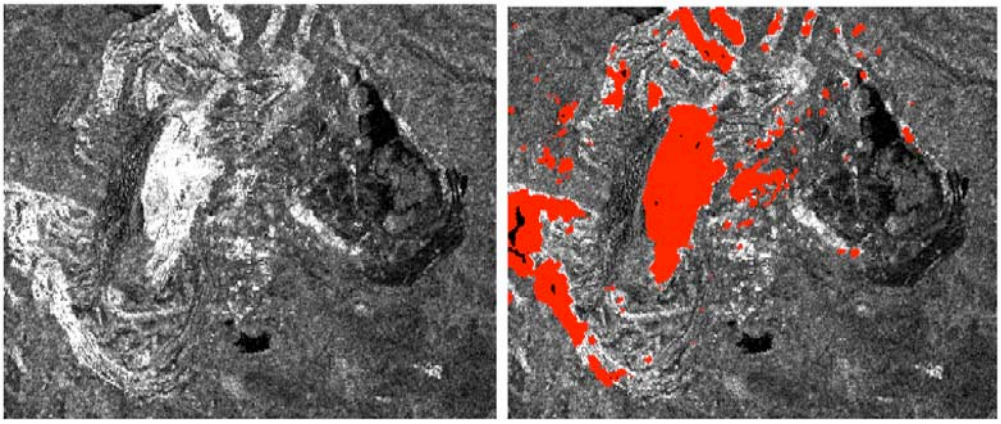

Figure 5: The results of Terrain Correction (left) and Layover Masking (right) using the SRTM DEM for the Argyle Diamond Mines

3. InSAR Processing

3.1 Data Selection

The long-term objective of the project (not considered here) was to provide help with tuning of a finite element model representing deformation of rock mass and with the analysis required for planning and design of the next mining phase. The main focus for this site was placed on the utilisation of available historical SAR data. The ESA archives listed only 10 ERS-2 SAR images for the particular mine site acquired after 2000. There was no SAR data covering the mine area available from other satellites, such as ENVISAT or ALOS. All of the ERS-2 data was acquired from the same path of a descending orbit, meaning that the radar was viewing in the (near) east to west direction. The available data is shown in **Table 1**.

Table 1: Available SAR scenes

Date	Orbit
2 Jan 2002	35041
18 Dec 2002	40051
22 Jan 2003	40552
26 Feb 2003	41053
2 Apr 2003	41554
7 May 2003	42055
11 June 2003	42556
17 March 2004	46564
21 April 2004	47065
13 Oct 2004	49570

From 10 SAR images it was possible to create 45 pairs for InSAR processing without considering number of linear independent combinations. However, not every pair is likely to result in an interferogram, and there are many reasons for this, mainly:

Images did not correlate due to temporal/surface changes,
Orbital separation (baseline) was too large,
Inconsistent instrument pointing causing decorrelation (dissimilar Doppler Centroids) was present.

The last reason above is a problem specific to the ERS-2 data. In 2000 ERS-2 suffered from gyro malfunctions and by the end of 2002 there were no operating gyros on the satellite.

Taking into account these limitations, the possible pairs were shortlisted to those that might result in an interferogram. Two main parameters were used in the selection process:

Orbital Baselines: The pairs that result in an orbital baseline greater than 400m were rejected as those with a larger baseline are not optimal for 2- and 3-pass InSAR methods.
Doppler Frequencies: Following recommendations from the European Space Agency, the pairs that have a difference in Doppler centroid frequency greater than 750 Hz were also rejected.

Table 2, 3 and **4** show the orbital baselines, Doppler Centroid separations and temporal baselines for all possible pairs. The pairs that match the specific criteria are highlighted in **Table 2** and **3**. Only six pairs matched both criteria and these are highlighted within **Table 4**.

Table 2: Orbital baselines of all pairs (m)

ORBIT	40051	35041	40552	41053	41554	42055	42556	46564	47065	49570
40051	0									
35041	447.3	0								
40552	1277.9	830.74	0							
41053	846.75	402.01	437.28	0						
41554	1342.1	895.3	79.505	507.96	0					
42055	769.96	322.77	508.38	102.67	573.03	0				
42556	788.84	342.01	489.89	68.386	557.23	36.388	0			
46564	844.38	401.75	444.79	22.039	517.26	115.95	79.912	0		
47065	633.5	186.49	644.8	216.99	710.75	138.08	155.54	218.97	0	
49570	446.09	80.045	842.63	406.08	911.57	342.66	354.33	401.47	206.04	0

Table 3: Doppler Centroid separations for all pairs (Hz)

ORBIT	40051	35041	40552	41053	41554	42055	42556	46564	47065	49570
40051	0									
35041	918.8	0								
40552	912.6	-6.2	0							
41053	2588.5	1669.7	1675.9	0						
41554	1164.6	245.8	252	-1423.9	0					
42055	1579.3	660.5	666.7	-1009.2	414.7	0				
42556	2435.2	1516.4	1522.6	-153.3	1270.6	855.9	0			
46564	1731.1	812.3	818.5	-857.4	566.5	151.8	-704.1	0		
47065	527.4	-391.4	-385.2	-2061.1	-637.2	-1051.9	-1907.8	-1203.7	0	
49570	-3407.9	-4326.7	-4320.5	-5996.4	-4572.5	-4987.2	-5843.1	-5139	-3935.3	0

Table 4: Temporal baselines of all pairs (days)

ORBIT	40051	35041	40552	41053	41554	42055	42556	46564	47065	49570
40051	0									
35041	350	0								
40552	35	385	0							
41053	70	420	35	0						
41554	105	455	70	35	0					
42055	140	490	105	70	35	0				
42556	175	525	140	105	70	35	0			
46564	455	805	420	385	350	315	280	0		
47065	490	840	455	420	385	350	315	35	0	
49570	665	1015	630	595	560	525	490	210	175	0

Of the six possible pairs, only three of them co-registered sufficiently well to create acceptable interferograms. This is most likely due to temporal ground changes between the two images. These pairs are summarised in **Table 5**. The temporal decorrelation is another factor limiting applicability of these methods.

Table 5: Description of the three acceptable pairs

Pair	Time Separation	Baseline
41554-40552	70 Days	79m
42556-41053	105 Days	68m
46564-42055	315 Days	115m

Since there are no common images between these three pairs, a DEM is required to derive the differential phase (i.e. 3-pass cannot be used here). These three pairs of images have been processed to identify possible ground deformation.

3.2 Layover mask

To generate the layover mask, the Shuttle Radar Topography Mission (SRTM) DEM (USGS, 2007) was used. Although the difference in date between the SAR images and the SRTM DEM was some three years, the results of the layover analysis seemed to agree very well with the image analysis. The original SAR image for the case study is shown in **Figure 6**, alongside the same image with the layover mask superimposed. This figure is presented such that the ERS satellite is viewing the terrain from the right hand side of the page. In the slant-range image, the layover region is small and clearly in a crescent-shaped area

on the left of the pit. The shape and position of the layover mask confirms that the SRTM DEM is sufficient to describe it.

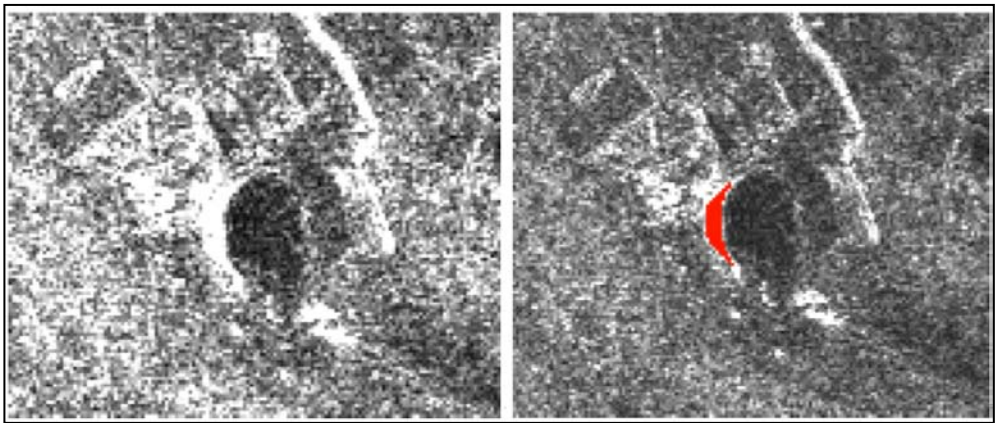

Figure 6: A slant range SAR image of Perseverance mine (left) and with layover area highlighted in red (right)

The terrain-corrected images are shown in **Figure 7**, where the input SAR image and the layover mask have been rectified to their proper shape and relative positions as would be seen on a map. It is clear that the rectification process has had a huge effect, considerably increasing the size of the layover area and decreasing the size of the Eastern wall of the pit. Much of the pit is obscured from view and the drastic effect of layover will clearly limit the available interferometric signal on the Western side of the feature.

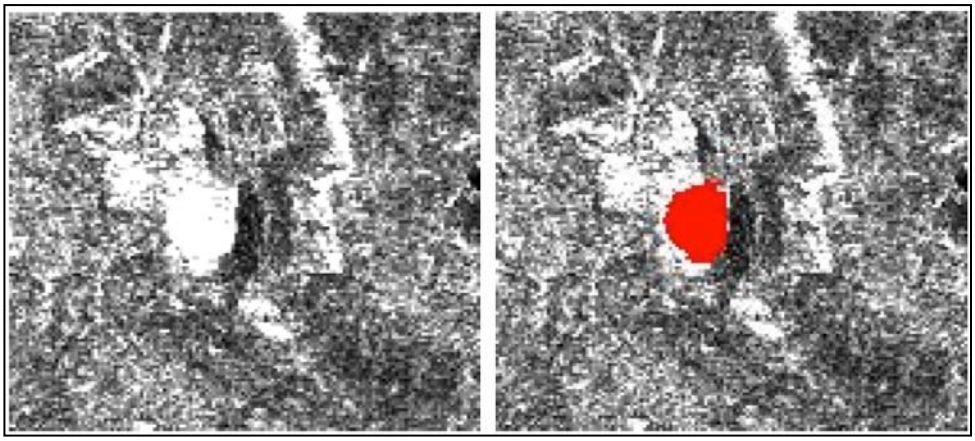

Figure 7: A geocoded SAR image of Perseverance mine (left) and with layover area highlighted in red (right)

3.3 Data Processing and Results

The data processing can be split up into the following main steps:

- Generation of real and simulated interferograms,
- Generation of the mask encompassing layover and pit,
- Generation of the differential phase and removal of any baseline trends,
- Derivation of the line-of-sight deformations,
- Georeferencing of the results into a suitable map projection.

The interferometric processing has been performed using the Doris interferometric processing software (Kampes and Usai, 1999) together with precise orbits (Scharroo et al., 1998) from the Delft Technical University. Phase unwrapping has been performed using the SNAPHU software from Stanford University (Chen and Zebker, 2001). The georeferencing and mask generation has been performed using in-house software. As described in previous section the high accuracy up-to-date DEM has been used as the terrain

model for the differential interferometry processing and for generation of the layover mask. The mask was applied to the data prior to phase unwrapping. By zero-weighting the phase data that corresponds to the mask, these regions should therefore have no effect on the neighbouring pixels. The mask is also applied to the final products so that erroneous measurements are not considered. However, the comparison of results generated with and without masking suggested that the applied mask made no significant difference to the InSAR results.

From the three pairs of SAR images (see **Table 5**), only two sets of results have been attained. This is due to one of the pairs being subject to severe atmospheric noise and hence rejected. The pair constructed from SAR images 42556-41053 (between February 2003 and June 2003) appeared to show what could be an atmospheric weather front in the vicinity of the mine area. An optical (AVHRR) image corresponding to the time of the ERS-2 overpass of 42556 also shows what could be this weather front (CSIRO, 2007). This is shown below in **Figure 8**. Due to significant difference in extend of weather front and deformation area, it may be possible to utilise the pair. However, the weather pattern contribution to phase noise required further detailed analysis.

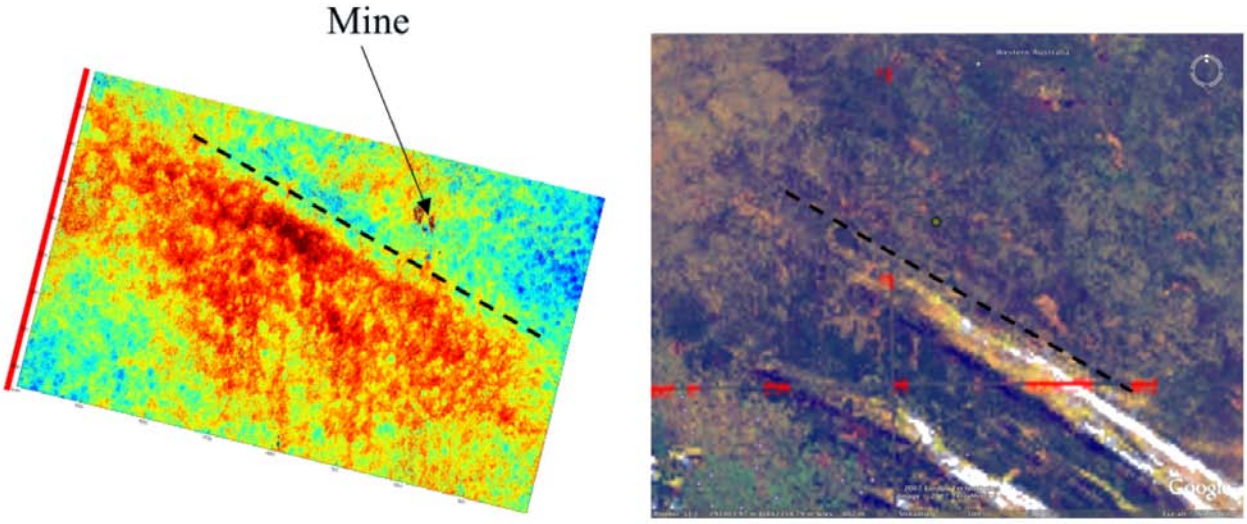

Figure 8: Georeferenced interferogram formed from SAR images 42556-41053 (left) and AVHRR image, representing cloud cover, from approximately same time as 42556 overpass (right) (CSIRO, 2007)

The masked line-of-sight deformation maps based on 46564-42055 and 41554-40552 pairs were generated and georeferenced into WGS84 latitude and longitude. The temporal baselines of the interferograms are 315 and 70 days respectively; this means that any deformation shown took place in this time period. All of the available data was acquired from the satellite descending orbits, meaning that the radar was viewing in the (near) east to west direction. This caused the west wall of the pit to be in an area of layover (see **Figure 5**). However the east wall of the pit was in a good view of the radar.

Little or no deformation has been identified from the 315-day interferogram, whereas a large deformation is seen for the 70-day interferogram. This appears contradictory but may be due to a signal ambiguity. The analysis of topographic changes, based on the historical topographical data (see Section 4.2), suggests a high amount of subsidence in 2003 equivalent to a linear rate of 6.0 m/yr or 16.4 mm/day in the southwest area of the pit. Over 70 days, between the SAR acquisitions, the vertical component of movement reached 1144 mm. Such change happened over a horizontal distance of 22.3 m, meaning that the change between neighbouring SAR pixels reached a similar value. Such a high rate of subsidence leads to ambiguity issues that cannot be resolved by InSAR processing. Any new processing technique, taking into account the dynamics of deformation field, must be developed and tested. The 70-day subsidence detected by InSAR, north of the pit is shown in **Figure 9-a**. In order to eliminate impact of local distortions on the far-reaching subsidence trough, a global polynomial was best fitted to the masked layer containing subsidence detected by InSAR. The applied mask eliminated the layover areas and the areas of known man-made terrain

disturbance. The best fit of a polynomial was characterised by: power = 3, mean error = $3.98e^{-5}$ m and RMS = 0.002451 (**Figure 9-b**).

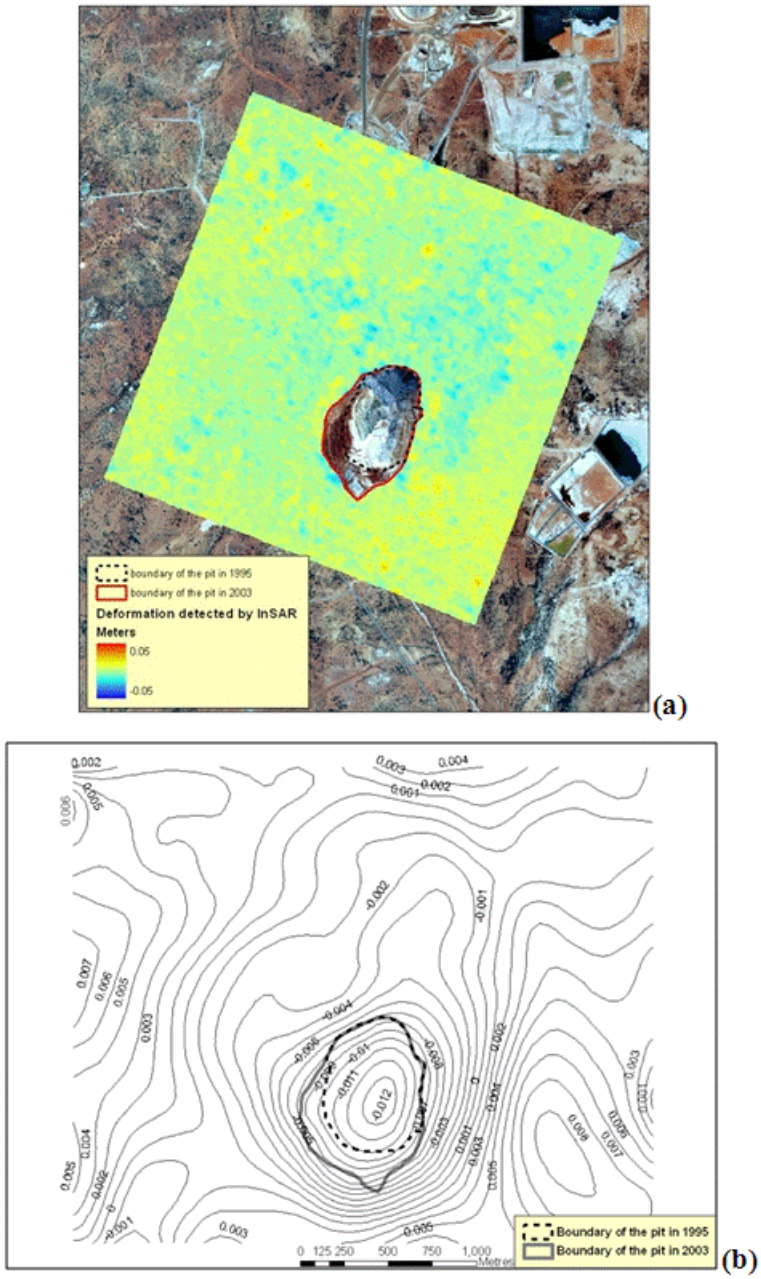

Figure 9: Subsidence detected by InSAR over Perseverance mine (over the period of 70 days)

4. Interpretation

4.1 Comparison with a subsidence analysis using classical surveys

The slope stability monitoring system initially included 71 points that were observed from the permanent theodolite station located on the top of waste dump and east of the open pit. Unfortunately, over time, a significant number of the reflectors were lost, reducing the value of the collected data in the subsidence active area. This area covered the southwest slope of the pit and the adjacent region southwest of the pit's crest. Replacement of the lost reflectors was not possible due to safety reasons (the area was classified as inaccessible). However, the network of monitoring points was expanded further towards the west, through

the establishment of 38 new monitoring stations. The locations of the monitoring stations are presented in **Figure 10**. The RTK GPS technology was used to monitor the movement at these new stations, providing relatively high positioning accuracy. A review of existing data suggests that the achieved positional accuracy was in the range of: ±1 mm (horizontal) and ±1 mm (vertical). A quality analysis of the GPS results and particularly a stability assessment of the GPS base station used for the surveys were not available.

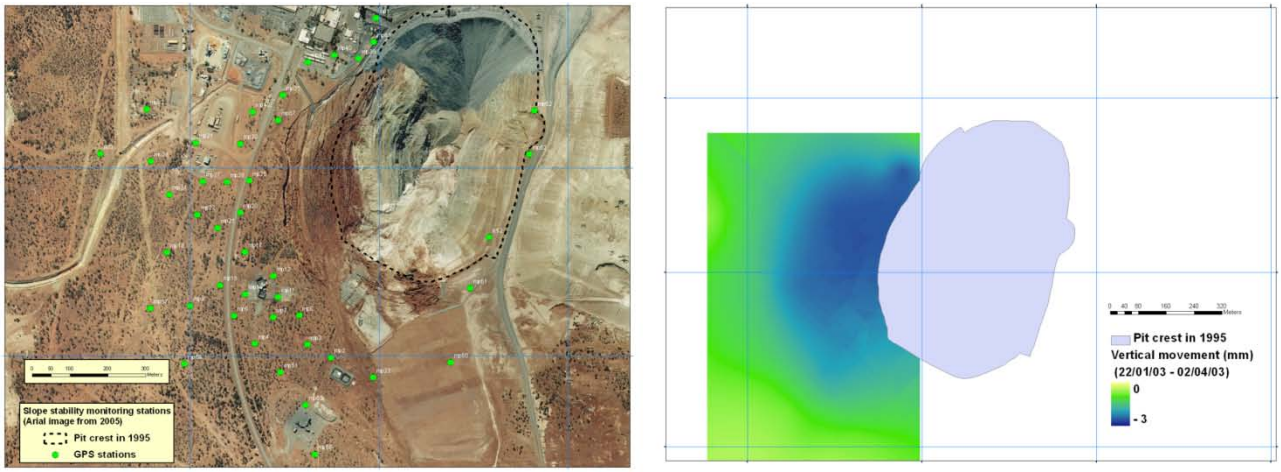

Figure 10: Slope stability monitoring stations and vertical movement between the dates of processed SAR acquisitions (41554-40552)

Using the deformation database, created by the 'Quick Slope' software, the three components of movement (dx, dy, dz), for each monitoring point, were extracted for the period between the acquisition dates of the SAR data. The extracted components were then used to approximate a continuous field of movements in the region west and southwest of the pit. It has to be noted that very small vertical movements, reaching the value of -3mm, were detected at the monitoring points during the period between the SAR acquisitions. A comparison between **Figure 9** and **Figure 10** shows that, unfortunately, the GPS survey did not cover the area of greatest deformation from the InSAR results. Also, the level of deformation detected is within a noise level of InSAR and only limited agreement was anticipated. According to Table 6.6, the obtained results suggest small agreement between GPS and InSAR results in their common area of coverage. The average difference is 2 mm and the standard deviation of differences is ±3 mm.

The InSAR results suggest existence of subsidence in this area, to the value between 0 and 10 mm, as a natural extension of the gentle subsidence trough detected to the north of the open pit. Considering the density of observations over a specific area, InSAR results can be better justified. However, it has to be noted that this comparison was performed over a limited area and a better agreement between both methods may exist elsewhere.

4.2 Mine Specific Deformation Analysis

4.2.1 Apparent Heave

The subsidence results obtained from the analysis of topographical surveys and from InSAR processing, suggested that some portions of the open pit slopes had experienced uplift (heave) not subsidence. Detailed analysis of the slope movement explained this phenomenon as not real but apparent uplift. It became clear that a change of elevation at any location is result of two components: vertical movement (subsidence) and horizontal shift of the ground. If these two movement components have an effect on a slope or a mining bench, and the horizontal movement acts toward the centre of a pit, it can result in an apparent heave of the ground (as shown in **Figure 11**).

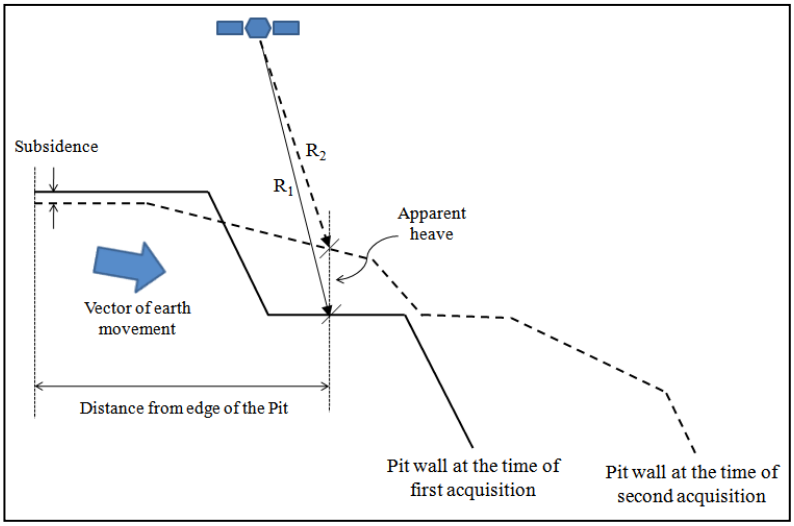

Figure 11: Apparent heave of the ground

4.2.2 Deformation Rates and the Issue of Ambiguity

The irregular rate, highly dynamic character of deformation induced by mining, may lead to an ambiguity issue. The ambiguity problem arises when high rate deformation occurs over a small area and happens when the vertical movement between the neighbouring cells (pixels) of the SAR image is greater than quarter of the wavelength of a radar signal. InSAR can only measure phase change as a fraction of a single wavelength and any motion that causes greater phase changes will still be given modulo one wavelength. This ambiguity cannot be resolved by InSAR processing procedures and techniques. Any further studies should take ambiguity issue into account since its appearance is very likely in case of high rate, dynamic deformation fields such as mining induced deformation.

In order to clarifying the importance of the deformation rate and the ambiguity issue in mining related applications of InSAR, six digital terrain models (DTM), based on topographical surveys (aerial photogrammetry), between 2001 and 2006 were used to determine the vertical component of movement (subsidence) that occurred between dates of topographical surveys. To remove systematic errors from individual DTMs, the common stable reference areas were selected and average elevations for each area were calculated. By comparing these average elevations, calculated for individual DTMs, the systematic component of elevation errors was determined and later removed from the calculated subsidence. The subsidence utilised the DTM from 2001 as the base. The examples of subsidence, spanning years 2001-2003 and 2001-2006, are presented in **Figure 12**.

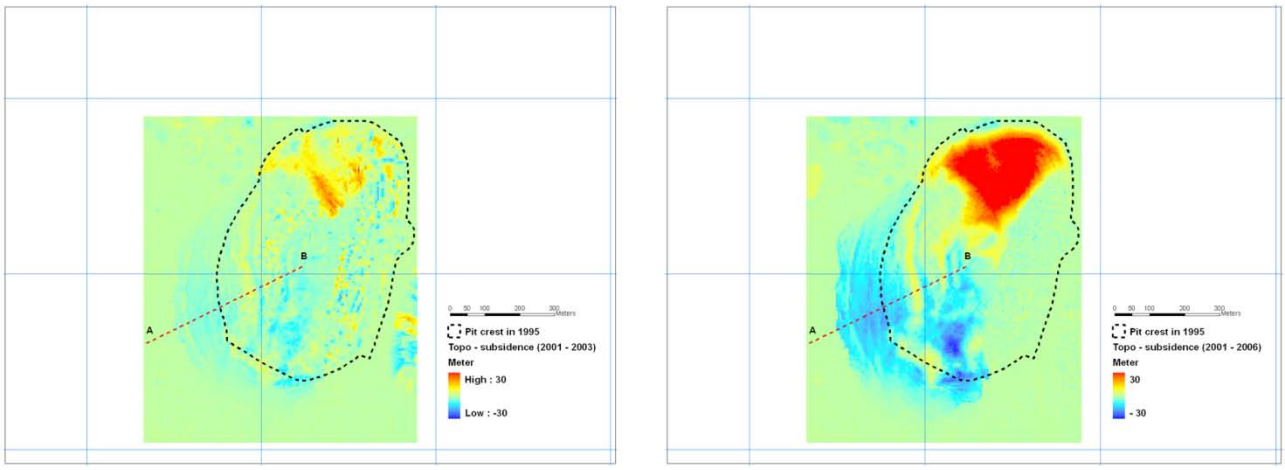

Figure 12: Subsidence between 2001-2003 and 2001-2006 derived from topo surveys for Perseverance mine

Figure 13 shows the series of cross-sections, representing the dynamics of ground movement along the profile A-B. It is clear that the area with greatest subsidence (south-west of the pit) experienced total of -17m of vertical movement between years 2001 and 2006, with the average yearly equivalent subsidence rate reaching -3.8m/yr (in 2005).

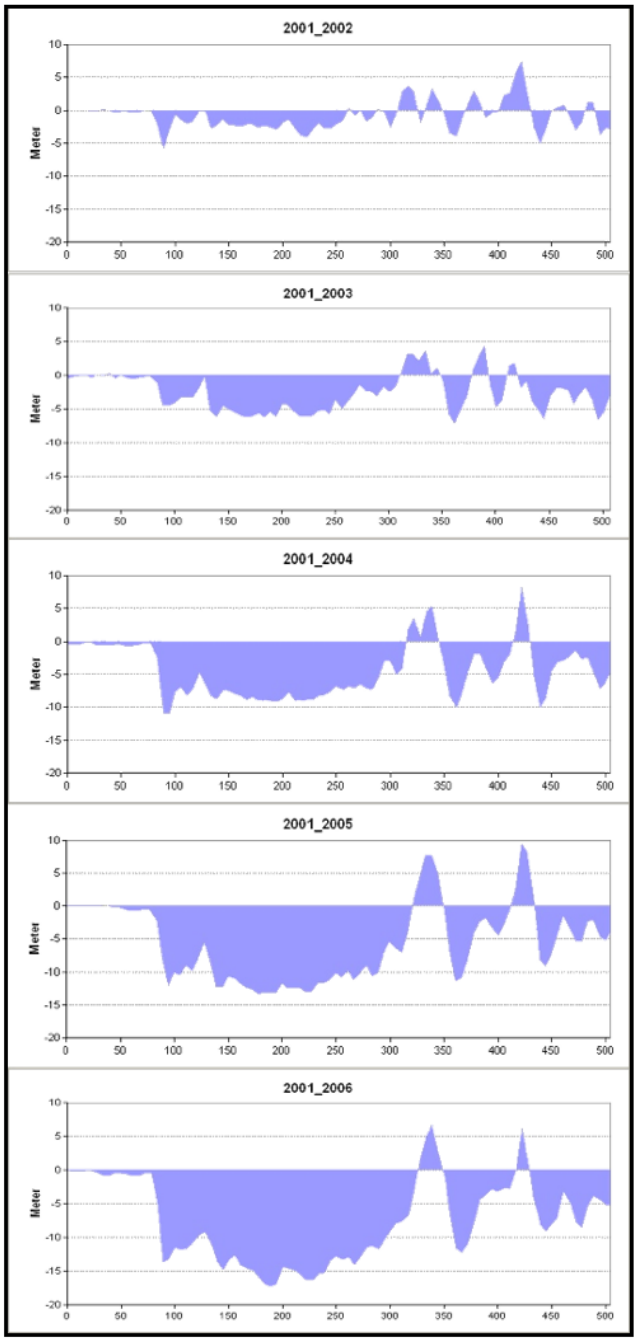

Figure 13: Subsidence along A-B cross-section referenced to 2001 DTM

Figure 14 shows the development of subsidence between 2001 and 2006. To eliminate inconsistency of detected local subsidence values represented by the individual pixels, the maximum rate was determined by averaging subsidence over an area of sixteen pixels (20m x 20m = 4x5m by 4x5m). The analysis suggests a high amount of subsidence during the period of SAR acquisitions that were used for processing (e.g. between 22/01/2003 and 02/04/2003). According to the values presented in **Figure 15,** the equivalent

subsidence rate has reached the level of 6.0 m/yr or 16.4 mm/day over the distance of 22.3 m, which definitely should lead to ambiguity issues in InSAR processing.

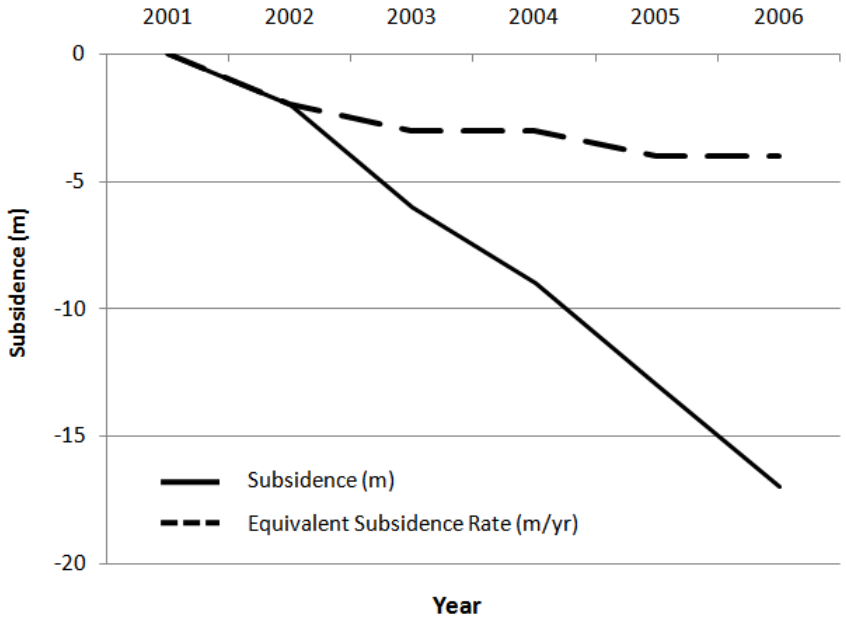

Figure 14: Development of subsidence between 2001 and 2006 calculated based on available DTMs

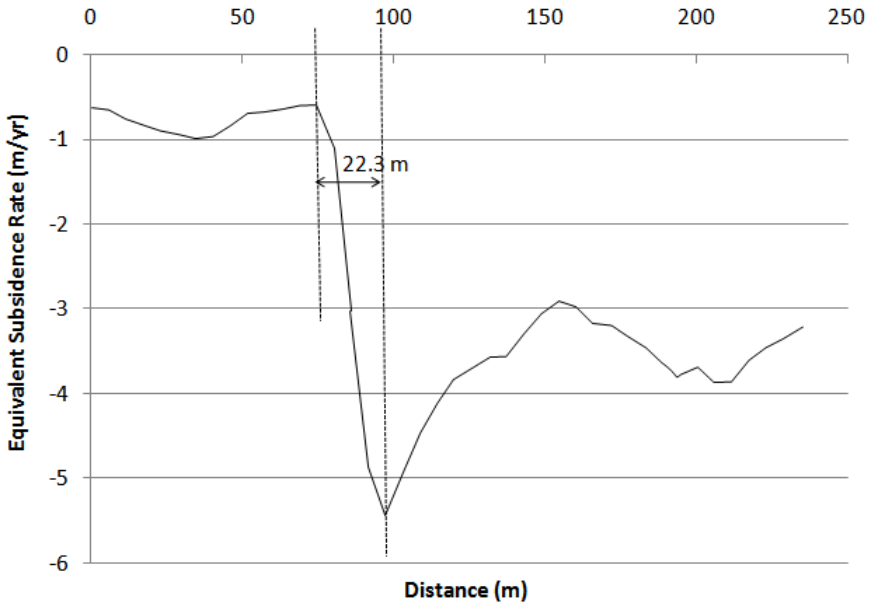

Figure 15: Equivalent subsidence rate in the period 2003-2004 along the profile A-B calculated based on available DTMs (from the point A to the edge of pit's crest; temporal baseline of 318 days)

5. Result Discussions and Conclusion

The InSAR method of subsidence monitoring uses a rapidly developing technology that offers many potential advantages. As a remote sensing method, it allows for monitoring of surface movement in the mining areas that are inaccessible due to their instability and cannot be monitored safely using the conventional monitoring techniques. However, the numerous parameters that impact on the accuracy and effectiveness of

the InSAR indicate that the method should be considered as experimental if applied to monitor high rate surface subsidence.

This paper includes the result of InSAR analyses for a mining operation in Western Australia. The very small number of archived SAR acquisitions available left authors without any choices regarding data selection. The geometry of the available data was also almost the worst possible for the application. All of the available data was acquired from the satellite descending orbits, meaning that the radar was viewing in the (near) east to west direction. This caused the west wall of the pit to be in an area of layover, which extended some distance past the edge of the pit. The other main issue affecting the studies was the unavailability of enough field data to validate InSAR results. The problem is: for a typical mining site most of the classical survey stations previously installed inside the deformation area will be lost or fall into the inaccessible area; also for areas outside of main deformation region, there is usually no classical survey stations installed since deformation monitoring over such areas not directly affects mine production. In case of Perseverance operation, available classical survey data covers only small portion of the deformation region; the comparative analysis of the InSAR results and classical GPS surveys suggest small agreement in their common area of coverage. However, considering the density of observations over a specific area, InSAR results can be better justified. Unfortunately, the authors did not have access to the quality analysis of GPS results and particularly to the stability assessment of GPS base station used for GPS surveys.

The analysis of historical topographic surveys allowed for the extraction of subsidence data spanning the period between 2001 and 2006. This analysis provided the subsidence inside the crater zone formed above the underground mining. That subsidence was characterised by large vertical and horizontal movements (few metres per year) leading to the development of significant discontinuities on the surface. A comprehensive analysis of ground deformation dynamics, based on topographical surveys has been discussed in order to study ambiguity issue associated with InSAR technique and its level of importance in mining related applications. It was recognised that such analyses provide basis for further adjustment of extend of poorly described areas by InSAR. The SNAPHU unwrapping algorithm used in this project is based on a minimum cost flow solution and therefore any localised subsidence effects that cause ambiguities may be lost if there is an obvious discontinuity within the neighbourhood of the subsiding area. This is the case for most of available unwrapping techniques. It was not possible to validate the unwrapping algorithm using ground truth since the area covered by ground control stations was relatively small and did not cover any significant deformation. Other surveying techniques such as laser altimetry can be considered as a resolution of InSAR ambiguity issue. However, considering the fact that monitoring deformation is not seen as a crucial component of mine production process, the cost of utilising such techniques practically precludes their application.

In addition to the subsidence analysis the research delivered important insight about application of InSAR remote sensing technique for monitoring of mining induced, localised, highly dynamic surface subsidence in the area of existing open pit mine with deep and steep slopes. The results show that layover is almost a certain occurrence in SAR images of open mines. However, with the chance to choose an incidence angle and prospect for the radar observation, and with knowledge of the terrain and the location of possible deformation, it would be possible to optimise acquisition of SAR images to minimise the layover and maximise the samples in the area of interest. The issues of layover and ambiguity are important aspects of acquisition planning and InSAR analysis if applied to mining areas.

Acknowledgement

The SAR acquisitions used in this research project were provided by the European Space Agency's (ESA) and were purchased from Eurimage. The in kind and financial support for this project was provided by BHPBilliton (Nickel West) and Argyle Diamond Mine.

References

- Chen, C.W., and Zebker, H.A., 2001. Two-dimensional phase unwrapping with use of statistical models for cost functions in non-linear optimisation. Journal of the Optical Society of America Vol. 18, 338-351.

- Ge, L., Change, M.H., Rizos C., 2004. Monitoring ground subsidence due to underground mining using integrated space geodetic techniques. Australian Coal Association Research Program (ACARP), project No C11029.

- Schreier, G., 1993. SAR Geocoding: data and systems. Wichmann Verlag, Karlsruhe.

- Kampes, B., Usai, S., 1999. The Delft Object-orientated Radar Interferometric Software. Proceedings of the 2nd International Symposium on Operational Remote Sensing. ITC, Enschede, The Netherlands, 16th August 1999.

- Lilly, P., Xu, D., Walker, P., 2000. Stability and risk assessment of pit Wallas at HP iron ore's Mt Whaleback mine. An Introductional Conference on Geotechnical & Geological Engineering. Melbourne, Australia, [CD-ROM].

- CSIRO, 2007. NOAA archive, Office of space science and applications, Earth observation centre, CSIRO. Australia. (Online) http://www.eoc.csiro.au/acres/perl/acresd.pl/

- Scharroo, R., Visser, P.N.A.M., Mets, G.J., 1998. Precise orbit determination and gravity field improvement for the ERS satellites. Journal of Geophysical Research. Vol. 103, C4. 8113-8127.

- USGS, 2007. Shuttle Radar Topography Mission, 3 Arc second scene SRTM. Global Land Cover Facility, University of Maryland, College Park, Maryland, February 2000.

- Wegmüller, U., Spreckels, V., Werner, C., Strozzi, T., Wiesmann, A., 2005. Monitoring of mining induced surface deformation using L-band SAR interferometry. IEEE International Geoscience and Remote Sensing Symposium, IGARSS '05. Proceedings. Vol. 3, 2165 – 2168.

- Farr, T. G., Rosen, P.A., Caro, E., Crippen, R., Duren, R., Hensley, S., Kobrick, M., Paller, M., Rodriguez, E., Roth, L., Seal, D., Shaffer, S., Shimada, J., Umland, J., Werner, M., Oskin, M., Burbank, D., And Alsdorf, D., 2007, The Shuttle Radar Topography Mission, Rev. Geophys., 45, RG2004, doi:10.1029/2005RG000183.